Available online at www.sciencedirect.com
SCIENCE DIRECT®
Marine Chemistry 97 (2005) 262–276
MARINE CHEMISTRY
www.elsevier.com/locate/marchem

Fabrication and test of sol–gel based planar oxygen optodes for use in aquatic sediments

Bettina König [a], Oliver Kohls [a], Gerhard Holst [a], Ronnie N. Glud [b], Michael Kühl [b,*]

[a] *Max-Planck-Institute for Marine Microbiology, Celsiusstr. 1, D-28359 Bremen, Germany*
[b] *Marine Biological Laboratory, Institute of Biology, University of Copenhagen, Strandpromenaden 5, DK-3000 Helsingør, Denmark*

Available online 14 July 2005

Abstract

We describe the fabrication of organically modified sol–gel (ORMOSIL) planar optodes for mapping the two-dimensional oxygen distribution in sediments. All sensor foils were based on the use of ruthenium(II)-tris-(4,7-diphenyl-1,10-phenantrolin)-perchlorate, which is a fluorescent dye quenched dynamically by oxygen. Sensors made with different sol–gel immobilisation matrices, different concentrations of precursors and indicator dye, as well as different types of scattering particles co-immobilised in the sensor foil were investigated systematically. Optimal sensor performance was obtained with dye concentrations of 2–10 mmol/kg in an immobilisation matrix made of diphenyldiethoxy-silan and phenyltriethoxy-silan precursors with addition of organically coated TiO_2 particles. The sensors exhibited a good mechanical stability and a high sensitivity from 0% to 100% oxygen, which remained constant over at least 36 days. The planar optodes were used with a fluorescent lifetime imaging system for direct mapping of the spatio-temporal variation in oxygen distribution within marine sediment inhabited by the polychaete *Hediste diversicolor*. The measurements demonstrated the spatio-temporal heterogeneity of the oxygen distribution in bioturbated sediments due to burrow structures and non-constant irrigation activity of the polychaete, which is difficult to resolve with microsensors or with traditional biogeochemical techniques.

Keywords: ORMOSIL; Planar oxygen optodes; 2D O_2 distribution; Bioturbation; Sediment; Polychaete; Worm burrow; *Hediste diversicolor*

1. Introduction

Optical sensors for oxygen, pH and CO_2 measurements in aquatic environments have been developed over the past 5–10 years and represent a good alternative to electrochemical sensors (Holst et al., 2000). In particular fiber-optic microsensors (microoptodes) for oxygen (Klimant et al., 1995) have been applied in biogeochemical studies for both laboratory and in situ measurements (e.g. Glud et al., 1999a; Wenzhöfer et al., 2000; Mock et al., 2002). However, microsensors allow only for a limited amount of point measurements that cannot fully resolve the inherent spatio-temporal heterogeneity in sediment structure and oxygen distribution, especially in bioturbated sediment. The recent development and application of optical sensor foils (planar optodes) and imaging systems

* Corresponding author. Tel.: +45 35321950.
E-mail address: mkuhl@bi.ku.dk (M. Kühl).

0304-4203/$ - see front matter © 2005 Elsevier B.V. All rights reserved.
doi:10.1016/j.marchem.2005.05.003

now enable microscale measurements of oxygen distribution in two dimensions (Glud et al., 1996; Holst et al., 1998, 1999; Liebsch et al., 1999). However, a detailed description of the production and evaluation of planar oxygen optodes is still lacking.

Optical oxygen sensors can be made with different oxygen sensitive dyes and immobilisation matrices causing differences in sensor response time, oxygen sensitivity, and photostability. Important design criteria for planar optodes to be used in environmental applications are (1) good hydrophobicity, (2) solid adhesion to the supporting foil, (3) homogeneity of the sensor foil, and (4) long-term stability against bleaching, ageing and biodegradation. Furthermore, the oxygen permeability of the applied immobilisation polymer is of major concern for the development of planar oxygen optodes.

Organically modified sol–gels (so-called *ORMOSIL*s) are transparent, tolerate high temperatures, and are not biodegraded. *ORMOSIL*s have previously been used as immobilisation matrix for various optical sensors (Iwamoto and Mackenzie, 1995; Lev et al., 1995; Shahriari et al., 1997), including well-functioning oxygen microsensors (Klimant et al., 1999). The sol–gel formation is based on (i) hydrolysis of the precursors, (ii) condensation and densification of the hydrolysed precursors, and (iii) drying of the matrix material. The properties of the resulting polymers are highly sensitive to environmental conditions like pH and temperature as well as the applied solvent. Furthermore, the choice of precursor affects the properties of the resulting sol–gels and numerous different types of organically modified sol–gels have been described in the literature (e.g. Liu et al., 1992; McEvoy et al., 1996). Phenyl-substituted precursors generally result in sensor foils with good hydrophobicity and a high photostability of the incorporated dye. The O_2 sensitivity of the sensor foils is mainly influenced by the hydrophobicity and the pore size of the matrix, both of which can be adjusted by varying the ratio of alkoxy- and phenyl-substituted groups of the precursors.

The measuring principle used with planar optodes is based on the dynamic quenching (Stern and Volmer, 1919; Kautsky, 1939) of ruthenium(II) 4,7-diphenyl-1,10-phenantroline (Ru-DPP) fluorescence by oxygen (Hartmann and Leiner, 1995). The oxygen dependent quenching can be quantified by a modified Stern–Volmer equation (Bacon and Demas, 1987; Carraway et al., 1991):

$$\frac{I}{I_0} = \frac{\tau}{\tau_0} = \left[\frac{a}{(1 + K_{SV} \cdot c)} + (1 - a)\right] \quad (1)$$

The equation shows the relation between oxygen concentration, c, the fluorescence intensity, I, and the lifetime, τ, respectively. The lifetime is defined as the average fluorescence lifetime of the excited state of the dye assuming mono-exponential decay. I_0 is the maximal fluorescence and τ_0 the lifetime in the absence of oxygen, K_{SV} is a constant expressing the quenching efficiency of the fluorophore, and a is the non-quenchable fraction of the fluorescence. Both K_{SV} and a are affected by the choice of the immobilisation polymer. The non-quenchable fraction can be considered constant for similar *ORMOSIL*s with similar dye concentration (Klimant et al., 1999). Once the calibration curves are obtained the parameter a in Eq. (1) can thus be determined for a particular *ORMOSIL*/dye mixture. Thereafter, two variable parameters remain in Eq. (1), i.e. K_{SV} and I_0 (or τ_0), and these can be determined from a simple two-point calibration (see details in Holst et al., 1998).

According to Eq. (1), optical oxygen measurements can be based on either fluorescence intensity or lifetime measurements. First applications of planar oxygen optodes were based on fluorescence intensity imaging (Glud et al., 1996). Fluorescence lifetime is, however, a more robust parameter for optical quantification of oxygen, as the measuring signal is independent of the absolute fluorescence intensity. Therefore some potential artefacts can be avoided (see also Holst et al., 1995, 1998) and transparent or semi-transparent planar optodes can be used (Holst and Grunwald, 2000). Fluorescence intensity based sensing often appears to have a better signal to noise ratio, but such measurements require a sensor layer that is oxygen permeable and optically dense (e.g. made of black silicone) leading to a slower response time and elimination of the possibility to observe the sample through the optode. However, the preferred measuring scheme depends on the given application (e.g. Glud et al., 1999b). Fluorescent lifetimes can be determined by phase-modulation techniques (Holst et al., 1995) or by direct determination of the fluorescence lifetime by measuring fluorescence in defined time windows after an excitation

light pulse (Holst et al., 1998). The lifetime imaging system used in this study uses the latter approach.

The goals of this study were (i) to develop and optimise planar optodes for oxygen, which are well suited for application in sediments, and (ii) to demonstrate the potential of the new planar optodes for studies in bioturbated marine sediments. We present detailed fabrication details and a systematic investigation of optodes made with various sol–gel materials. Optimised planar optodes were used for measurements of oxygen dynamics around a *Hediste diversicolor* burrow in coastal marine sediment.

2. Material and methods

2.1. Synthesis of ORMOSILs

Three different *ORMOSIL* matrices were fabricated from silicon alkoxide- and organylalkoxy-silanes precursors with one to three oxide-bound functional groups. The precursors were converted to *ORMOSIL*s via acid catalyzed hydrolysis and poly-condensation reactions (Fig. 1), followed by a temperature controlled densification process (Brinker, 1988).

The first series of *ORMOSIL*s were prepared from the precursors diphenyldiethoxy-silan (DDOS; Merck, Germany) and trimethoxymethyl-silan (denoted as TOMS; Merck, Germany) with an increasing concentration of TOMS versus DDOS (Table 1). A known amount of DDOS (denoted *m* in Table 1) was added to 6.42 ml Ethanol (0.11 mol) and 2.1 ml 0.1 N Hydrochloric Acid (0.21 mmol) (Merck, Germany), which acted as a catalyst (Liu et al., 1992; Klimant et al., 1999). In all experiments, the solution became turbid upon catalyst addition but then turned transparent after a few minutes. Subsequently, the solution was quickly heated to 60 °C under reflux condensation for 120 min. The temperature stabilized at 60 °C ± 3 °C within 5 min after the reflux was started. Special care was taken to obtain homogeneous solutions by applying rigorous stirring. After the heating was stopped various amounts of TOMS (denoted *x* in Table 1) were added followed by further stirring at room temperature for 30 min. The solution was then poured into deionized water and left for phase separation at room temperature overnight. The following day, the viscous polymer oil was separated and dried at 200 °C. The drying process was stopped after 24 h, and the cold sol–gel was pulverized before further use.

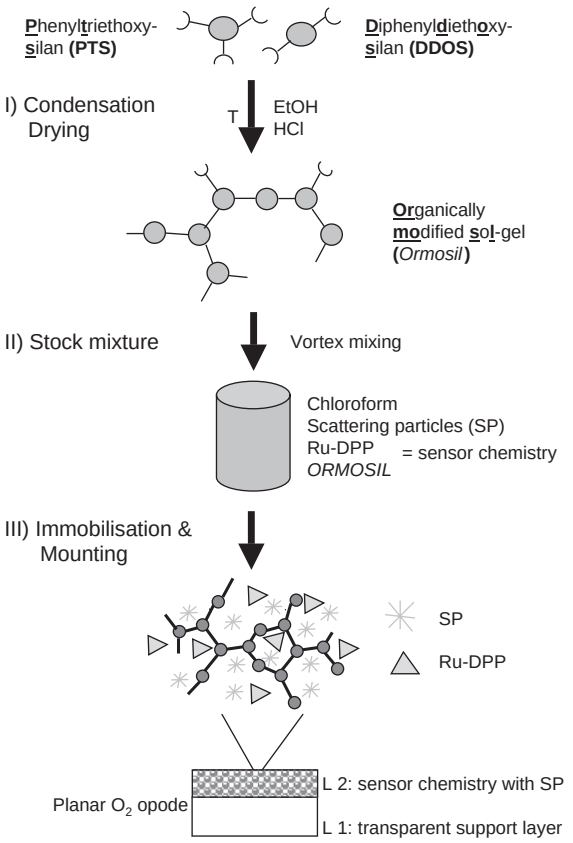

Fig. 1. Scheme for the synthesis of *ORMOSIL* based planar O_2 optodes: (I) Condensation and drying of the precursors PTS and DDOS. (II) Stock mixture preparation consisting of the solvent chloroform, scattering particles (SP), the fluorescence dye (Ru-DPP), and the *ORMOSIL*. (III) Immobilisation of the sensor chemistry (=L2; final thickness after hardening ~10 μm), and mounting on a transparent support layer (=L1; thickness ~100 μm).

A second series of *ORMOSIL*s was made with phenyltriethoxysilan (PTS; Merck, Germany) and methoxytrimethysilan (MOTS; Merck, Germany) under identical experimental conditions concerning amount of solvent, catalyst, heating and drying conditions, as used in the first series (Table 2). Additionally, the effect of using different reflux times, i.e. 30, 60 or 90 min, was studied.

Finally, a third series of *ORMOSIL* matrices were made from the two components DDOS and PTS with increasing ratios of PTS to DDOS (Table 3). In this case the two precursors were added at once and

Table 1
Composition of the *ORMOSIL* series 1 matrices

OMS type no.	DDOS	TOMS	TOMS/DDOS
	Mass		Molar ratio (mol TOMS/mol DDOS)
	m (mmol)	*x* (mmol)	$\underline{x}$
1.1	25.3	0	0
1.2	25.0	0.6	0.02
1.3	25.0	1.0	0.04
1.4	28.4	3.1	0.11
1.5	28.4	5.0	0.18
1.6	16.7	3.4	0.20
1.7	25.0	7.0	0.28
1.8	25.0	9.6	0.38

The precursors diphenyldiethoxysilane (DDOS) and trimethoxysilan (TOMS) were used to synthesize the organically modified sol–gel series 1 (OMS 1). In the second and third columns the experimental concentrations are given while the last column contains the TOMS/DDOS molar ratio.

dissolved in 5.83 ml ethanol (0.1 mol). Thereafter, 2.3 ml 0.1 N HCl (0.23 mmol) was added under vigorous stirring. The reflux time and temperature were the same as in series 1. Although nothing was added to the solution after the heating was stopped, the solution was stirred for 20 min at room temperature. The final steps were undertaken under identical conditions as in series 1.

Table 2
Composition of the *ORMOSIL* series 2 matrices

OMS type no.	PTS	MOTS	MOTS/PTS	Reflux time
	Mass		Molar ratio (mol MOTS/mol PTS)	
	m (mmol)	*x* (mmol)	$\underline{x}$	
2.1	25.0	0	0	
2.2 a	26.0	1.8	0.07	30 min
2.2 b	26.0	1.8	0.07	60 min
2.2 c	26.0	1.8	0.07	90 min
2.2 d	26.0	1.8	0.07	120 min
2.3	25.0	2.5	0.10	
2.4	26.0	3.6	0.14	
2.5	25.0	5.0	0.20	
2.6	26.0	7.3	0.28	

The second series of *ORMOSIL*s (OMS 2) were prepared from phenyltriethoxysilan (PTS) and methoxytrimethylsilan (MOTS). The reflux time was varied for the fabrication of OMS 2.2. In the second and third columns the experimental concentrations are given while the last column contains the MOTS/PTS molar ratio.

Table 3
Composition of the *ORMOSIL* series 3 matrices

OMS type no.	PTS	DDOS	PTS
	Mass		Molar ratio (mol DDOS/mol DDOS+PTS)
	m (mol)	*x* (mol)	$\underline{m}$
3.1	25.0	0	1
3.2	22.6	2.5	0.9
3.3	20.0	5.0	0.8
3.4	17.6	7.5	0.7
3.5	15.1	10.0	0.6
3.6	12.5	12.5	0.5
3.7	9.9	14.9	0.4
3.8	7.5	17.6	0.3
3.9	5.0	20.0	0.2
3.10	2.5	22.7	0.1
3.11	0	25.3	0

The third series of *ORMOSIL*s (OMS 3) were fabricated from the two components diphenyldiethoxysilan (DDOS) and phenyltriethoxysilan (PTS). In the second and third columns the experimental concentrations are given while the last column contains the molar ratio of PTS to the base of the molar sum of DDOS and PTS. The DDOS ratio is given by one minus the PTS ratio.

2.2. Synthesis of the oxygen indicator dye

225.9 mg $RuCl_3$*H_20 (Fluka, Germany) were diluted in 5 ml ethylene-glycol (Fluka, Germany) and 0.5 ml de-ionized water, and then heated to 160 °C under reflux condensation. At 120 °C 1.06 g of the ligand 4,7-diphenyl-1,10-phenantrolin (also known as bathophenantrolin; Fluka, Germany) was added. The mixture was heated for another 45 min, cooled, and then 50 ml acetone (Fluka, Germany) was poured into the cold solution. The mixture was filtered through a G4 glass filter and the filtrate then contained the ligand-substituted ruthenium complex. To precipitate the ruthenium complex as a perchlorate salt, 50 ml perchloric acid (1 N; Fluka, Germany) were added to 10 ml of the filtrate. Finally, the ruthenium complex salt was re-crystallized to gain pure ruthenium (II) tris (4,7-diphenyl-1,10-phenantrolin) perchlorate (denoted as Ru-DPP). A more detailed description of the synthesis is given elsewhere (Klimant, 1993; Klimant et al., 1999).

2.3. Preparation of planar oxygen optodes

Planar optodes with and without light scattering particles (denoted as SP) incorporated in the

dye–*ORMOSIL* matrix were fabricated. A stock sensor solution was prepared by dissolving varying amounts (0.4–16.5 mg) of Ru-DPP and 250 mg *ORMOSIL* in 1 ml chloroform (Merck, Germany). After addition of scattering particles, the mixture of sensor solution and scattering particles was homogenized by Vortex mixing for 2 h (Klimant et al., 1999).

Oxygen sensors based on *ORMOSIL* 3.2 were fabricated with dye concentrations of 1, 2, 5, 10, 20, and 50 mmol/kg, respectively, in order to identify the optimal dye concentration for planar optodes. Furthermore *ORMOSIL* 3.10-based planar optodes were fabricated with different types of scattering particles made of TiO_2 (Merck, Germany), $BaSO_4$ (Merck, Germany), lipophilized $BaSO_4$, Pigment A (coated TiO_2, Kronos, Germany), or Pigment B (coated TiO_2, Kronos, Germany) in order to find the optimal type of scattering material.

Planar optodes were fabricated by spreading the sensor cocktail on a 125 μm thick transparent polyester foil (Mylar, Goodfellow, Great Britain) (for a schematic drawing, see Fig. 1). For this, the polyester foil was fixed to a flat stainless steel plate by generating vacuum from below. The sensor cocktail was then applied to the foil and spread in a thin layer using a sharp knife-like metal device. The layer thickness was regulated with spacers so that the knife moved ~100 μm over the surface of the foil. After evaporation of the solvent (at least 24 h at room temperature) the sensor layer had a final thickness of approximately 10 μm.

2.4. Characterization of planar oxygen optodes

Measuring characteristics of the planar optodes were determined by calibration measurements in water flushed with defined mixtures of nitrogen and oxygen. Two-point calibrations were performed from readings within air saturated water and N_2 flushed water. For first characterizations of the optodes, we used a fiber-optic instrument for measuring fluorescent lifetimes via the phase-modulation method (described in Holst et al., 1995). With this method, the dye in the planar optode is excited with sinusoidal modulated light and therefore emits sinusoidal modulated light with a certain delay. The delay causes a shift in the phase angle (ϑ) between excitation and emission allowing the determination of the lifetime (see below). The applied setup consisted of a two-phase lock-in amplifier (Stanford Research Instruments, SR 830, USA), which controlled both the excitation source (a 470 nm LED, Nichia, Japan, equipped with a Schott BG12 glass filter) and the detector (a photodiode, Hamamatsu/S5821-01 equipped with a Schott OG590 glass filter). Light was guided to and from the planar optode via a bifurcated optical fiber (AMS Optotech, Germany). The emitted fluorescence signal was referenced to a red-colored foil (fire red, Conrad Electronics, Germany). After analogue and digital signal processing, the oxygen dependent fluorescence signal was recorded as a phase angle, i.e. the phase shift between the two sinusoidal signals. From this phase angle, ϑ, and the modulation frequency, f (here 45 kHz), the fluorescence life time, τ, was calculated according to

$$\tau = \frac{\tan(\vartheta * \pi / 180)}{2 * \pi * f} \quad (2)$$

A more detailed characterization of sensor foils was done with a modular luminescence lifetime imaging system (described in Holst et al., 1998). The experimental set-up (Fig. 2) consisted of a fast gateable CCD camera (SensiMod VGA, PCO, Germany) and a blue excitation light source, which was either an array of 8 blue light emitting diodes (470 nm LED, DCL Components Ltd., UK) or a Xenon flash lamp (Oxygen Enterprises, USA). Homogeneous illumination of the planar optode was realized with a fiber optic ring light (Schölly Fiberoptic GmbH, Germany) coupled to the excitation light source. The ring light was mounted in a light-tight housing in front of the camera and connected to the light source via a fiber-optic cable (Hartmann and Ziegler, 1996; Holst et al., 1998). In this study, the images covered an area of 2.6×2.5 cm^2, corresponding to a spatial resolution of 50×50 μm^2 per pixel. However, the spatial resolution can easily be changed by modification of the optical configuration in front of the CCD camera. A pulse-delay generator (SRS-DG535, Stanford Research, USA) controlled the triggering of excitation light and image acquisition. All instruments were controlled by custom-made software (see Holst and Grunwald, 2000). Image analysis and calibration were done with self-made programs in the software package IDL (Research Systems Inc.,

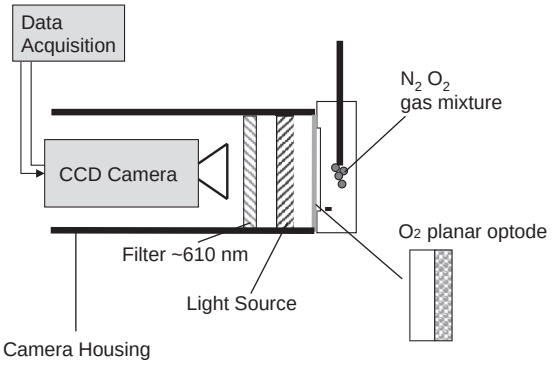

Fig. 2. Schematic drawing of the imaging system with camera housing, filter, light source and data acquisition device. The experimental chamber equipped with an O_2 planar optode was flushed with defined mixtures of N_2 and O_2. The walls of the chamber were darkened.

USA). A detailed description of the data acquisition and post-processing procedures are presented elsewhere (Holst and Grunwald, 2000).

2.5. Measurements of O_2 distribution around worm burrows

The planar optodes with the best measuring characteristics were used to make measurements of O_2 distribution in sediment surrounding burrows of the polychaete *H. diversicolor*. The sediment and small specimens of *H. diversicolor* were retrieved from Helsingør Harbour, Denmark. The sediment was sieved and transferred to a self-made flow chamber ($4 \times 100 \times 40$ mm) equipped with a planar oxygen optode (Fig. 3). The planar optode covered an area of 2.6×2.5 cm^2 yielding a pixel resolution of approximately 50×50 μm^2. The flow chamber was mounted in front of the camera housing and was shielded against ambient light on all other sides in order to prevent stimulation of photosynthetic oxygen production and optical interferences. Aerated water kept at constant salinity (30) and temperature (23 °C), was circulated at constant flow velocity through the flow chamber during the experiments. One specimen of *H. diversicolor* was added to the flow chamber and the polychaete was allowed to establish a burrow and to acclimate to the experimental conditions overnight before pictures of the oxygen distribution were recorded.

The experiments were performed with 3 different specimens of *H. diversicolor*. The polychaetes were kept for 2–3 days in the chambers without feeding in order to limit bacterial growth within the chamber and tubing, which would affect the O_2 measurements. With every specimen up to 10 trials were performed with intervals of 1 min, 2 min, 3 min, and 10 min between the images. The trials lasted from 10 min to 3 h. The images presented here show the most spectacular events.

The diffusive oxygen uptake (DOU) was calculated from O_2 images by Fick's first law of diffusion. According to Fick's first law of diffusion the vertical flux of O_2 through the sediment surface, J_V can be calculated as

$$J_V = -\phi^* D_S^* \left(\frac{\partial C(z)}{\partial z} \right) \quad (3)$$

where ϕ is the porosity (here 0.34 vol/vol) of the sediment, D_S is the tortuosity, temperature and salinity corrected diffusion coefficient for O_2 in the sediment (Ullman and Aller, 1982; Broecker and Peng, 1974; Li and Gregory, 1974), and $(\partial C/\partial z)$ is the vertical gradient of O_2 just below the sediment surface. Eq. (3) was also used to estimate the horizontal O_2 flux through the burrow wall (J_H) from horizontal oxygen gradients. These calculations assume steady state conditions around the burrow walls for the moment images were taken.

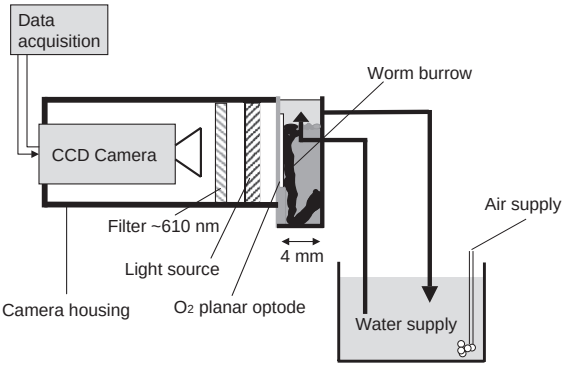

Fig. 3. Schematic drawing of the imaging system with camera housing, filter, light source and data acquisition device. The experiment chamber equipped with an O_2 planar optode was filled with sediment inhabited by one specimen of *N. diversicolor*. The chamber was constantly supplied with fresh aerated seawater at constant temperature and salinity. The walls of the chamber were darkened.

3. Results and discussion

3.1. Influence of precursor concentration on quenching and mechanical properties of optodes

Precursors and reaction conditions were partly chosen based on the findings of Carraway et al. (1991) and Murtagh et al. (1998). Their studies demonstrated that Ru-DPP exhibits improved quenching by oxygen when immobilised in materials of increasing hydrophobicity and oxygen permeability. Additionally, the increase of methyl groups in the *ORMOSIL*s leads to a better O_2 sensitivity at lower O_2 concentrations. Nevertheless, it was difficult to foresee the final polymerisation products. In case of the *ORMOSIL* series 1–3, the solvent concentration was high compared to the precursor concentration promoting intra-molecular reactions leading to cyclic and short molecule chains (Hoshino and Mackenzie, 1995). Furthermore, aromatic groups can improve the photostability of oxygen-sensing materials and phenyl-substituted *ORMOSIL*s enhance the solubility of the Ru-DPP dye in the matrix (Klimant et al., 1999). Phenyl groups do not participate in the polymerisation process and they need more steric space than alkoxy groups leading to a less dense network formation in the *ORMOSIL* matrix.

We took advantage of these effects in our fabrication of optimised planar O_2 optode with high sensitivity. One measure of O_2 sensitivity is the signal width, i.e. the difference between $\tau(0)$ and $\tau(\text{air})$, of a planar oxygen optode, where $\tau(0)$ and $\tau(\text{air})$ denote the luminescence lifetime in oxygen free and fully aerated water, respectively. The signal width depends on the O_2 permeability of the polymer matrix and a steep slope in the calibration curve indicates a high O_2 permeability (Liu et al., 1992). The O_2 signal width is also reflected in the lifetime ratio, $R = \tau(0)/\tau(\text{air})$ (Fig. 4). For every stock solution of sensor material (see Section 2.4) two similar planar optodes were prepared and characterized and each of these optode represent a single data point in Fig. 4.

In the *ORMOSIL* series 1 material, DDOS had two hydroxy-groups capable of polymerisation. This promoted the formation of linear chains and the addition of a 'cross-linker' such as TOMS caused the formation of larger interconnected structures resulting in weak glass like polymers exhibiting a low O_2 sensitivity. Increasing the amount of interconnections (by increasing amounts of TOMS) yielded a harder polymer matrix but did not increase the O_2 sensitivity. No significant change in R was observed with O_2 sensors prepared from the *ORMOSIL* series 1 with varying molar ratios of the precursors (Fig. 4A; Table 1). The R-values varied only between 1.1 and 1.2 although the amount of the 'cross-linker' TOMS was increased from 0 to 0.4 mol TMOS/mol DDOS. However, the

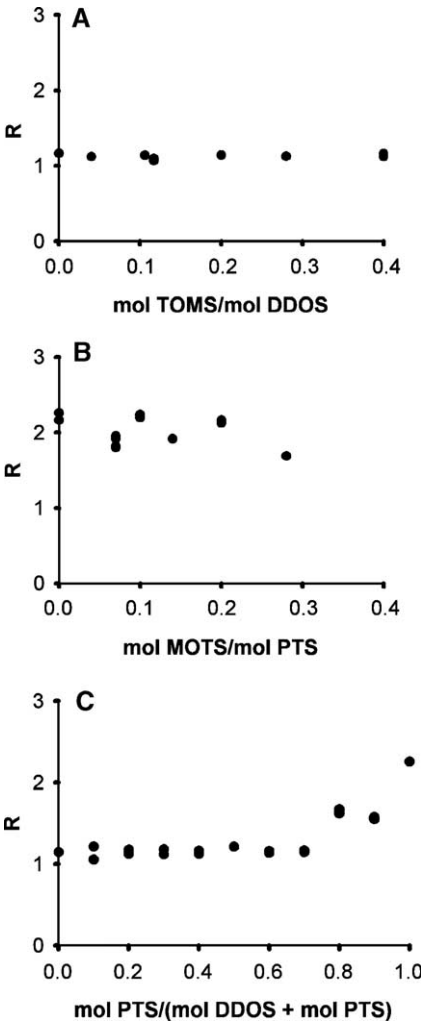

Fig. 4. Impact of the precursor molar ratio on R-values of the *ORMOSILS* 1–3: (A) precursor TOMS relative to DDOS molar ratio prepared as presented in Table 1, (B) precursor MOTS relative to PTS molar ratio prepared as presented in Table 2, (C) precursor PTS relative to DDOS molar ratio as presented in Table 3. The R-values were measured with a decay time based imaging technique.

optodes with high amounts of TOMS became more brittle and less adhesive to the supporting foil. One reason for this could be the progressed self-condensation of DDOS, which reduces the chance for TOMS to form interlinks between the DDOS polymers. Thus the resulting molecule and matrix structures were not changed in their basic appearance. It is also likely that TOMS reacted with itself and formed its own dense structure, which fills in the larger structure of the DDOS polymers. This could also explain the low O_2 sensitivity.

The O_2 optodes prepared from the *ORMOSIL* series 2 were expected to show a decrease in their O_2 sensitivity with increasing molar ratio of MOTS yet were also expected to have a less brittle structure and show better adhesion to the support foil. Indeed, the optodes changed from a hard glassy consistency to a soft polymer structure with increasing amounts of MOTS. The results presented in Fig. 4B show a minor decrease of R (and thus in the O_2 permeability) from 2.2 to 1.7 with this increase in the amount of MOTS. MOTS functions as 'end-cap' (Liu et al., 1992; Klimant et al., 1999) for the self-condensation of PTS and interrupts the polymerisation. The relatively low amounts (Table 2) of MOTS used here (Table 2) lead to an enhanced number of free alkoxyl groups, allowing for continued condensation reactions in the planar oxygen optodes. This then causes drift of the calibration curve over time after fabrication (data not shown).

We studied the impact of varying reflux time on the measuring characteristics of O_2 optodes made of the OMS 2.2 matrix. It was observed that R increased from 1.4 to 1.8 with increasing reflux time (30–120 min) during the sol–gel preparation (Table 4). The short reflux time of 30 min resulted in a soft polymer with a poor oxygen solubility. Longer reflux times (60–120 min) increased the formation of cross-links during the polymerisation resulting in a more open net-like structure with improved oxygen solubility. A reflux time of 120 min resulted in planar optodes with good R-values and this timing was used for all further *ORMOSIL* preparations. Although the optodes of *ORMOSIL* series 2 exhibited a much better oxygen permeability ($R>1.7$) than those made of the *ORMOSIL* series 1 ($R<1.2$), the solubility of *ORMOSIL* 2 in chloroform was poor, and the manufactured planar optodes suffered from a poor mechanical stability.

Table 4
The role of reflux time for OMS 2.2 performance

OMS type no.	t (min)	R
2.2 a	30	1.41
2.2 b	60	1.54
2.2 c	90	1.68
2.2 d	120	1.80

Planar oxygen optodes were fabricated on the base of OMS 2.2, prepared under different reflux times, and characterized by their decay time ratio, R.

Another approach was to moderate the *ORMOSIL* properties via mixing the precursors DDOS and PTS without later supply of an 'end-cap' or 'cross-linker' (*ORMOSIL* 3 material). Previous studies showed that pure DDOS forms weak polymers with a low O_2 sensitivity, whereas pure PTS forms a brittle glass with a good O_2 sensitivity. By using a mixture of the two precursors we could fabricate planar oxygen sensors with both a high O_2 sensitivity and a stable polymer matrix. The optodes prepared from the *ORMOSIL* series 3 (Fig. 4C) exhibited a significant increase of R at >0.7 mol fractions PTS. With pure PTS, the value of R almost doubled from 1.2 to 2.2. The *ORMOSIL* 3 materials generally had a good solubility in chloroform and exhibited a good mechanical stability. Based on the mentioned observations, the *ORMOSIL* 3.2 ($R=1.6$) (see Table 3) was selected as the most promising matrix material for planar optodes. Tests of planar optodes made of this *ORMOSIL* showed very good sensor performance for >36 days (see below).

3.2. Role of scattering particles for planar optode performance

The addition of scattering particles to the sensing layer can enhance the signal intensity of planar optodes, as the fluorescent indicator is excited more efficiently due to increased scattering in the matrix. Furthermore, scattering particles can facilitate a more even excitation of the foil if the particles are dispersed homogeneously in the sensor material. However, too large amounts of TiO_2 in the sensor matrix can cause significant fluorescence quenching due to a charge transfer process between Ru-DPP and TiO_2 (Matthews et al., 1997). Four different types of scattering particles were investigated with respect to their dispersion in

ORMOSIL 3.2 and the homogeneity of the final oxygen optode (Fig. 5). As a measure of homogeneity, we calculated the mean and standard deviation of the fluorescent intensity values of all pixels in images recorded with the optode in air-saturated water (Fig. 5). The most homogeneous sensors were manufactured with the Kronos pigments A and B yielding a symmetrical peak with a low standard deviation of 1.3 (Fig. 5C+D). It was not possible to detect a significant difference in performance between the two pigments. In comparison, the optodes prepared with uncoated $BaSO_4$ (Fig. 5A) and TiO_2 (Fig. 5B) exhibited non-symmetrical distributions of fluorescence intensity with a standard deviation of 3.7 and 1.7, respectively. Besides facilitating good dispersion and homogeneous sensor foils, the organic coating of the Kronos pigments apparently also minimized the quenching effect of TiO_2 mentioned above. Although a high homogeneity was reached, it was not possible to use average calibration values for the entire planar optode, and it was still necessary to perform a pixel-by-pixel calibration, when the planar optodes were applied with the imaging system. This means that every pixel of the O_2 concentration image corresponds to a specific area (here approximately 50×50 μm^2) of the planar optode, which must be regarded as a local sensor with its corresponding calibration values. Consequently, the experimental setup must not be modified after calibration or, alternatively, precise position markers have to be set on the optodes to enable re-adjustment of the images during data processing.

3.3. Dye concentration and ageing of planar optodes

The performance of 3 sensors made with *ORMOSIL* 3.2 and (Ru-DPP) concentrations of 2, 10 and 50 mmol/kg matrix polymer, respectively, was investigated over 36 days (Fig. 6). The best performance with respect to both O_2 sensitivity and long-term stability of the sensor was observed with planar optodes containing a low indicator concentration of 2 mmol/kg matrix material (Fig. 6A). The calibration curves of the two other sensors showed less oxygen sensitivity and the curves changed significantly over

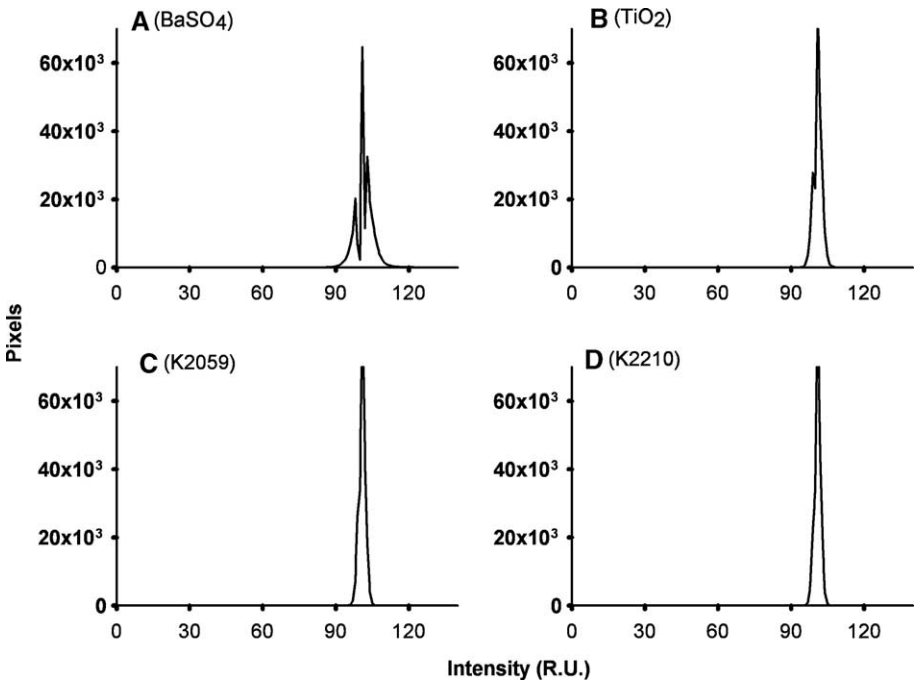

Fig. 5. Histograms of pixel intensity values as a measure of sensor homogeneity. The applied *ORMOSIL* was 3.2 with a dye concentration of 5 mmol/kg. Results from planar optodes prepared with different types of scattering particles: (A) $BaSO_4$, (B) TiO_2, (C) K2059 and (D) K2210. The mean intensity of each image was set to 100%.

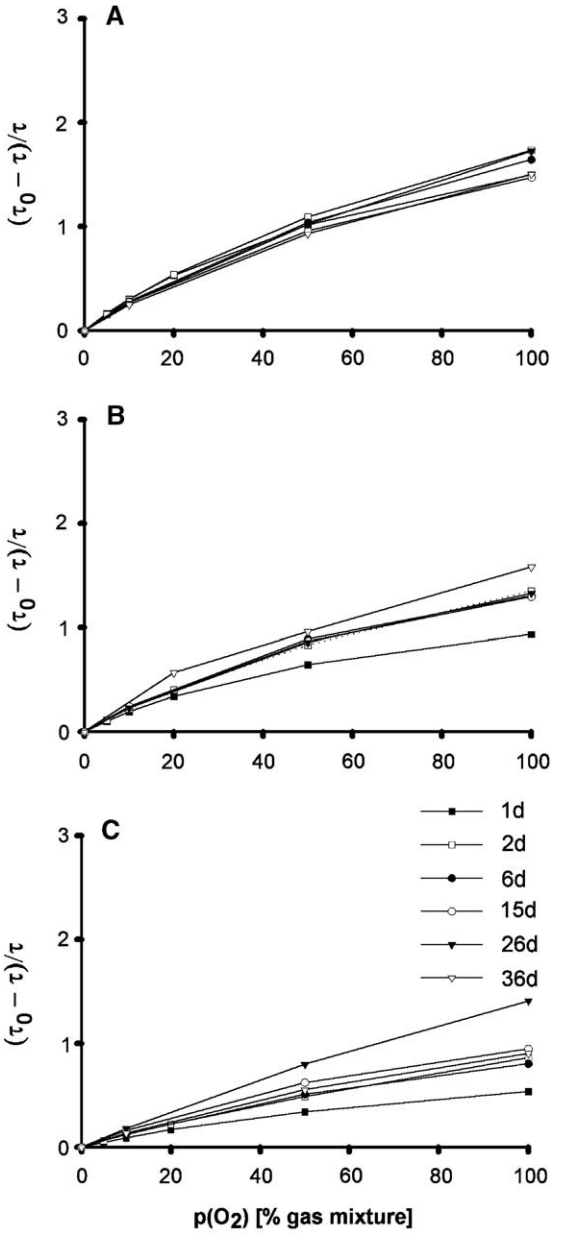

Fig. 6. Calibration curves from planar oxygen prepared of *ORMOSIL* 3.2 with dye concentrations of (A) 2 mmol /kg, (B) 10 mmol/kg and (C) 50 mmol/kg at varying ageing stages. The calibration curve is given as ratio of τ_0/τ normalized to zero versus the O_2 concentration.

time (Fig. 6B,C). For long-term applications in sediments we thus found *ORMOSIL* 3.2-based sensors with Kronos pigment A scattering particles and a dye concentration of ~2–10 mmol/kg matrix material to be optimal. At higher dye concentrations photodegradation increases and products thereof can quench the fluorescence (Klimant et al., 1999).

3.4. Reproducibility of planar optode fabrication

Three sets of *ORMOSIL* 3.2-based planar optodes with Kronos pigment A were fabricated and calibrated under identical conditions (Fig. 7). While properties like mechanical stability, long-term stability of calibration, and adhesion were indifferent between the foils, it was difficult to produce polymers with absolute identical physical properties with respect to O_2 permeability. Thus, it was not possible to obtain a large batch of sensor foils with identical calibration curves. This may, however be achieved by a more advanced setup for coating the carrier foil. Especially at high partial pressure of oxygen the calibration curves for different foils deviated from each other, while the performance in the range of 0% to 20% O_2 was relatively uniform. Overall, the reproducibility was sufficient for our needs but it is important to carefully calibrate each individual sensor foil. All calibration curves showed an excellent correlation with the modified Stern–Volmer equation (Eq. (1)).

The main difference between our procedure and the *ORMOSIL* preparation process described by Klimant et al. (1999) was the use of a lower drying and

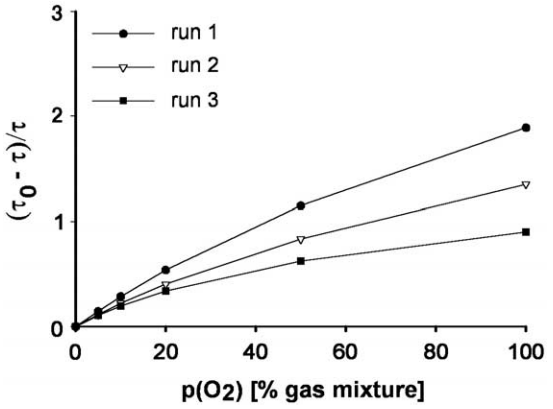

Fig. 7. Calibration curves of planar oxygen optodes based on 3 preparation trials of *ORMOSIL* 3.2 with a dye concentration of 5 mmol/kg. The calibration curve is given as ratio of τ_0/τ normalized to zero versus the O_2 concentration.

curing temperature, which simplifies the preparation of the *ORMOSIL*s. Furthermore, our systematic investigation showed that reflux times of up to 120 min during fabrication resulted in *ORMOSIL* matrices with improved oxygen solubility and that addition of organically coated TiO_2 yielded more homogeneous planar optodes.

3.5. Mapping of the two-dimensional O_2 distribution around polychaete burrows

A laboratory application of *ORMOSIL* 3.2-based planar optodes allowed direct mapping of the two-dimensional O_2 distribution around a worm burrow (Fig. 8). We show here a time series of 4 images obtained with a time delay of 3 min between each image. A more detailed study of oxygen dynamics around *H. diversicolor* burrows in natural and artificial sediments is presented elsewhere (König et al., in preparation). The images reflect the two-dimensional oxygen distribution (expressed in a linear colour table) around the outlet branch of a U-shaped tube inhabited by one individual. Since the flow chamber was larger in width than the diameter of the worm burrow, part of the burrow was not build completely parallel to the measuring plane. The effect is visible in all images of Fig. 8, where the burrow appears to be interrupted. Furthermore, the images showed no pronounced heterogeneity of oxygen in the sediment except around the worm burrow, as the sediment was sieved and homogenized before being introduced to the experimental chamber.

The oxygen penetration depth at the primary sediment–water interface varied between 2 and 3.8 mm and was affected by the presence of a diffusive boundary layer (DBL) closely following the sediment surface. However, the polychaete frequently left its tube causing a rearrangement of the sediment surface. The outline of the burrow and the sediment surface could be traced by illuminating the flow chamber from the opposite side of the planar optode coated chamber causing a detectable shadow relief which could be detected by the camera system.

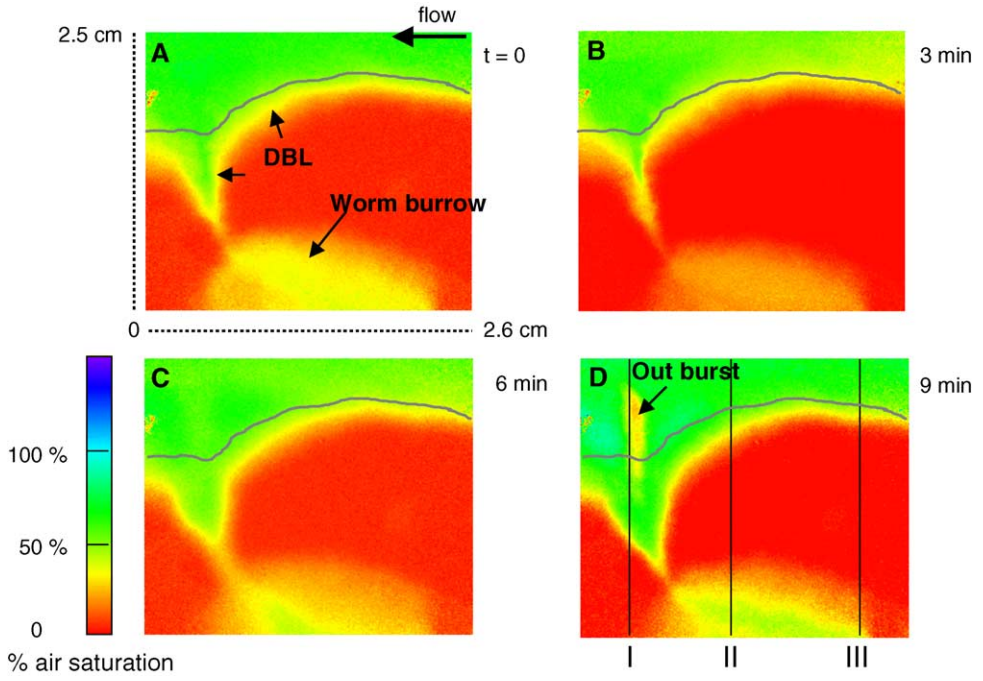

Fig. 8. Time series (3 min intervals) recording of the oxygen distribution around a *Hediste diversicolor* burrow (presented in a linear color scale). They thick grey line indicates the sediment surface. The flow of the overlaying water was directed from the right to the left. The positions of the 3 profiles presented in Fig. 9 are indicated in the last image.

During the shown image sequence (Fig. 8), the O_2 level inside the burrow and in the outlet oscillated between 60% and 5% air saturation. The last image of the sequence shows an outburst of water with low oxygen content from the burrow (see arrow in Fig. 8D) after a period of less irrigation activity. The O_2 fluctuations over time in the burrow were due to variations in the pumping activity of the polychaete causing the oxygen concentration to vary from 0% to 60% or even 90% (not shown) air saturation within a few minutes. Three characteristic oxygen profiles (Fig. 9) were extracted from Fig. 8D (as indicated by vertical lines). Profile I was strongly affected by an outburst of oxygen-depleted water (~19% air sat.), and by the presence of the burrow opening. Profiles II and III showed the diffusive oxygen uptake at the primary sediment–water interface and enhanced levels of oxygen deep in the sediment due to radial diffusion of oxygen from the burrow, i.e., the secondary sediment–water interface. Our data show that planar optodes have a large potential for resolving the oxygen dynamics in bioturbated sediments at a hitherto unreached spatio-temporal resolution (Kristensen, 2000). With this technique it is possible to visualize the oxygen distribution and dynamics both at the primary sediment–water interface and at the secondary interface present around worm burrows, and to calculate fluxes and specific oxygen consumption activities at these interfaces.

Images of the vertical O_2 flux (Fig. 10A and C) were obtained by applying Eq. (3) to the O_2 images of Fig. 8A and D making no differentiation in the flux directions. In order to increase the signal to noise ratio of the flux calculations 3×3 neighbouring pixels were averaged. Consequently, the spatial resolution of the calculated O_2 flux images was reduced to 150 μm per pixel. The DOU indicated by the vertical flux at the primary sediment surface reached at maximum of 4.7 mmol m^{-2} day^{-1}. Images of the horizontal oxygen flux were also calculated (Fig. 10B and D). Maximal horizontal oxygen fluxes of up to 7.9 mmol m^{-2} day^{-1} were calculated at the burrow wall. At the primary sediment–water interface no significant horizontal flux was observed. These O_2 fluxes are relative low compared to the reported fluxes of 18–27 mmol m^{-2} day^{-1} (Fenchel, 1996; Pelegri and Blackburn, 1995) and 52.8 mmol m^{-2} day^{-1} (Banta et al., 1999) and this could be due to the manipulation of the sediment prior to experiments. The O_2 uptake of the primary and secondary sediment–water interface were in the same order of magnitude as, e.g. reported by Fenchel (1996). The oxygen flux images presented in Fig. 10 show highest O_2 fluxes along the primary and secondary sediment–water interfaces. Such data obtained in combination with other measures of the

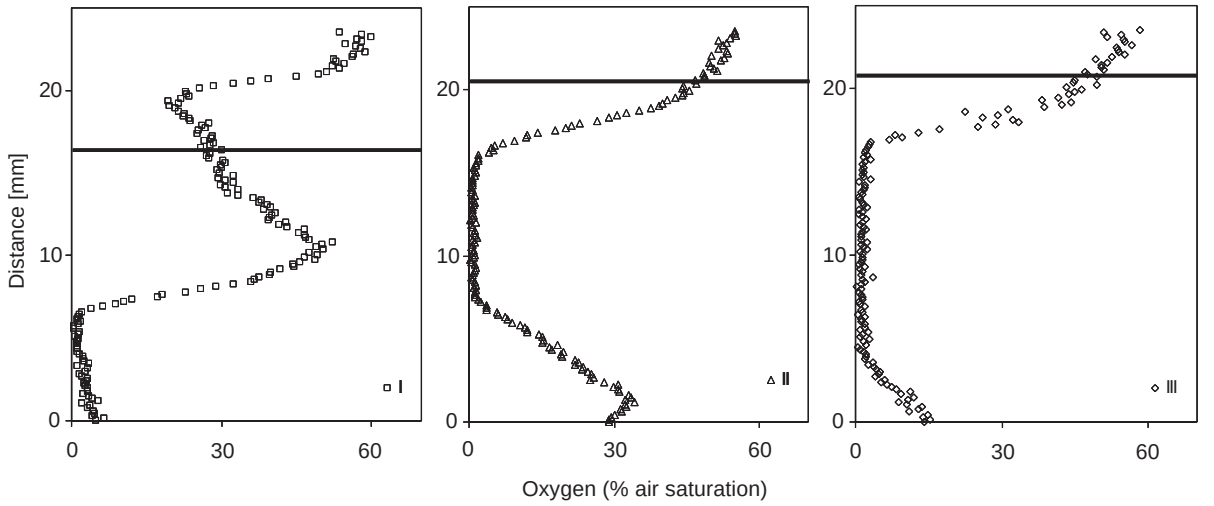

Fig. 9. Concentration profiles extracted from Fig. 8D. The sediment surface is indicated with the black line. Profile I is dominated by the outburst of water with low oxygen content from the worm burrow. Profiles II and III both show evidence of O_2 diffusion across the sediment–water interface and radial diffusion from the burrows, although profile II clearly shows a stronger effect of radial diffusion.

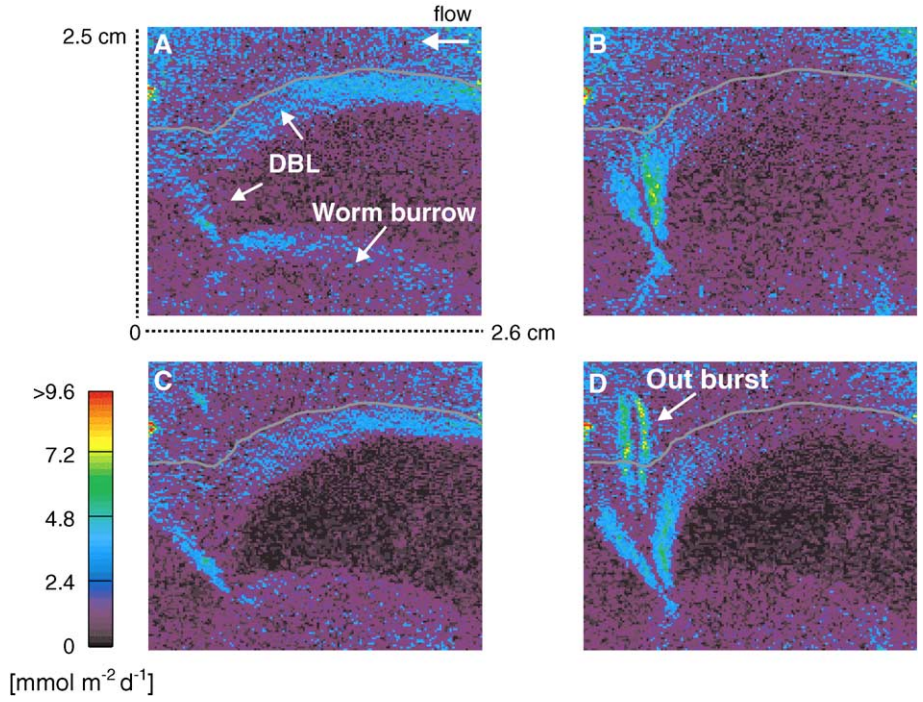

Fig. 10. The vertical and horizontal distribution of O_2 flux expressed in a linear color scale. In order to increase the signal to noise ratio the spatial resolution was reduced to 150 μm. The thick grey line indicates the sediment surface. Panels A and C show the distribution of vertical O_2 flux (derived from Fig. 8A and D), whereas panels B and D show the horizontal O_2 flux. In all panels no indication on the direction of the fluxes is given.

sediment biogeochemistry such as, e.g. total oxygen uptake, oxygen microsensor measurements, measurements of polychaete biomass and irrigation activity, and precise determination of burrow geometry now enable the construction of a precise oxygen budget for bioturbated sediments (see, e.g. Wenzhöfer and Glud, 2004). Here we have focussed on describing the fabrication and performance of planar optodes. A detailed study of the oxygen dynamics in sediments inhabited by *H. diversicolor*, based on the use of planar optodes, microsensors and mini-flow sensors, will be presented elsewhere (König et al., in preparation).

4. Summary

We developed planar oxygen indicator foils (planar optodes) well suited for environmental application in aquatic systems. This study is to our knowledge the first to present a detailed description of planar optode fabrication along with a more systematic investigation of important variables affecting planar optode performance. It is our hope that these details will help make the technique more accessible. We demonstrated the first use of planar oxygen optodes for investigating the oxygen dynamics around polychaete burrows in sediments. With planar oxygen optodes and the corresponding imaging system, the spatial and temporal O_2 dynamics in bioturbated marine systems can now be investigated at a hitherto unreached level of resolution in the laboratory and even in situ by use of a recently developed underwater instrument for planar optodes (Glud et al., 2001; Wenzhöfer and Glud, 2004).

Acknowledgements

This study was financed by the European Commission (MICROFLOW, CT970078; PHOBIA, QLK3-CT-2002-01938), the Max-Planck-Society (Germany), and the Danish Natural Science Research Council.

References

Bacon, J.R., Demas, J.N., 1987. Determination of oxygen concentrations by luminescence quenching of a polymer-immobilized transition-metal complex. Analytical Chemistry 59, 2780–2785.

Banta, G.T., Holmer, M., Jensen, M.H., Kristensen, E., 1999. Effects of two polychaete worms, *Hediste diversicolor* and *Arenicola marina*, on aerobic and anaerobic decomposition in sandy marine sediment. Aquatic Microbial Ecology 19, 189–204.

Brinker, C.J., 1988. Hydrolysis and condensation of silicates: effects on structure. Journal of Non-Crystalline Solids 100, 31–50.

Broecker, W.S., Peng, T.-H., 1974. Gas exchange rates between air and sea. Tellus 26, 21–35.

Carraway, E.R., Demas, J.N., DeGreff, A., Bacon, J.R., 1991. Photophysics and photochemistry of oxygen sensors based on luminescent transition-metal complexes. Analytical Chemistry 63, 337–342.

Fenchel, T., 1996. Worm burrows and oxic microniches in marine sediments: 1. Spatial and temporal scales. Marine Biology 127, 289–295.

Glud, R.N., Ramsing, N.B., Gundersen, J.K., Klimant, I., 1996. Planar optrodes: a new tool for fine scale measurements of two-dimensional O_2 distribution in benthic communities. Marine Ecology. Progress Series 140, 217–226.

Glud, R.N., Klimant, I., Holst, G., Kohls, O., Meyer, V., Kühl, M., Gundersen, J.K., 1999a. Adoption, test and in situ measurements with O_2 microopt(r)odes on benthic landers. Deep-Sea Research I 46, 171–183.

Glud, R.N., Kühl, M., Kohls, O., Ramsing, N.B., 1999b. Heterogeneity of oxygen production and consumption in a photosynthetic microbial mat as studied by planar optodes. Journal of Phycology 35, 270–279.

Glud, R.N., Tengberg, A., Kühl, M., Hall, P., Klimant, I., Holst, G., 2001. An in situ instrument for planar O_2 optode measurements at benthic interfaces. Limnology and Oceanography 46, 2073–2080.

Hartmann, P., Leiner, M.J.P., 1995. Luminescence quenching behaviour of an oxygen sensor based on a Ru(II) complex dissolved in polystyrene. Analytical Chemistry 67, 88–93.

Hartmann, P., Ziegler, W., 1996. Lifetime imaging of luminescent oxygen sensors based on all-solid-state technology. Analytical Chemistry 68, 4512–4514.

Holst, G., Grunwald, B., 2000. Luminescence lifetime imaging with transparent oxygen optodes. Sensors and Actuators. B, Chemical 64, 1–13.

Holst, G., Kühl, M., Klimant, I., 1995. A novel measuring system for oxygen microoptodes based on a phase modulation technique. SPIE Proc. Conf. Chem., Biochem. and Enviro. Fibre Sensors, pp. 2508–2545.

Holst, G., Kohls, O., Klimant, I., König, B., Kühl, M., Richter, T., 1998. A modular luminescent lifetime imaging system for mapping oxygen distribution in biological samples. Sensors and Actuators. B, Chemical 51, 163–170.

Holst, G., Grunwald, B., Klimant, I., Kühl, M., 1999. A luminescent lifetime imaging system using imaging fibres to measure the 2D distribution of O_2 in biological samples. Proceedings of SPIE 3860, 154–163.

Holst, G., Klimant, I., Kohls, O., Kühl, M., 2000. Optical microsensors and microprobes. In: Varney, M. (Ed.), Chemical Sensors in Oceanography. Gordon & Breach, pp. 143–188.

Hoshino, Y., Mackenzie, J.D., 1995. Viscosity and structure of Ormosil solutions. Journal of Sol-Gel Science and Technology 5, 83–92.

Iwamoto, T., Mackenzie, J.D., 1995. Ormosil coatings of high hardness. Journal of Materials Science 30, 2566–2570.

Kautsky, H., 1939. Quenching of luminescence by oxygen. Faraday Society 35, 216–219.

Klimant, I., 1993. Entwicklung optischer Sauerstoffsensoren auf der Basis luminiezierender Übergangsmetallkomplexe, PhD thesis, University Graz, Austria.

Klimant, I., Meyer, V., Kühl, M., 1995. Fibre-optic oxygen microsensors, a new tool in aquatic biology. Limnology and Oceanography 40, 1159–1165.

Klimant, I., Ruckruh, F., Liebsch, G., Stangelmayer, A., Wolfbeis, O., 1999. Fast response oxygen micro-optodes based on novel soluble Ormosil glasses. Mikrochimica Acta 131, 35–46.

König, B., Glud, R.N., Kühl, M., in preparation. Oxygen dynamics around *Nereis diversicolor* burrows as studied with planar optodes.

Kristensen, E., 2000. Organic matter diagenesis at the oxic/anoxic interface in coastal marine sediments, with emphasis on the role of burrowing animals. Hydrobiologia 426, 1–24.

Lev, O., Tsionsky, M., Rabinovich, L., Glezer, V., Sampath, S., Pankratov, I., Gun, J., 1995. Organically modified sol–gel sensors. Analytical Chemistry 67, 22–30.

Li, Y.-H., Gregory, S., 1974. Diffusion of ions in sea water and in deep-sea sediments. Geochimica et Cosmochimica Acta 38, 703–714.

Liebsch, G., Klimant, I., Wolfbeis, O.S., 1999. Luminescent lifetime temperature sensing based on sol–gels and poly(acrylnitrile)s dyed with ruthenium metal-ligand complex. Advanced Materials 11, 1296–1299.

Liu, H.-Y., Switlaski, S.C., Coltrain, B.K., Merkel, P.B., 1992. Oxygen permeability of sol–gel coatings. Applied Spectroscopy 46, 1266–1272.

Matthews, L.R., Avnir, A., Modestov, A.D., Sampath, S., Lev, O., 1997. The incorporation of titania into modified silicates for solar photodegradation of aqueous species. Journal of Sol-Gel Science and Technology 8, 619–623.

McEvoy, A.K., McDonagh, C.M., MacCraith, B.D., 1996. Dissolved oxygen sensor based on fluorescence quenching of oxygen-sensitive ruthenium complexes immobilized in sol–gel-derived porous silica coatings. Analyst 121, 785–788.

Mock, T., Dieckmann, G., Haas, C., Krell, A., Tison, J.L., Belem, A., Papadimitriou, S., Thomas, D.N., 2002. Micro-optodes in sea ice: a new approach to investigate oxygen dynamics during sea ice formation. Aquatic Microbial Ecology 29, 297–306.

Murtagh, M.T., Shahriari, M.R., Krihak, M., 1998. A study of the effects of organic modification and processing technique on the luminescence quenching behavior of sol–gel oxygen sen-

sors based on a Ru(II) complex. Chemistry of Materials 10, 3862–3869.

Pelegri, S.P., Blackburn, T.H., 1995. Effect of bioturbation by *Nereis* sp., *Mya arenaria* and *Cerastoderma* sp. on nitrification and denitrification in estuarine sediments. Ophelia 42, 289–299.

Shahriari, M.R., Murtagh, M.T., Kwon, H.C., 1997. Ormosil thin films for chemical sensing platforms. Proceedings of SPIE 3105, 40–51.

Stern, O., Volmer, M., 1919. Über die Abklingungszeit der Fluoreszenz. Physikalische Zeitschrift 20, 183–188.

Ullman, W.J., Aller, R.C., 1982. Diffusion coefficients in nearshore marine sediments. Limnology and Oceanography 27 (3), 552–556.

Wenzhöfer, F., Glud, R.N., 2004. Small-scale spatial and temporal variability in benthic O_2 dynamics of coastal sediments: impact of fauna activity. Limnology and Oceanography 49, 1471–1481.

Wenzhöfer, F., Holby, O., Glud, R.N., Nielsen, H.K., Gundersen, J.K., 2000. In situ microsensor studies of a shallow water hydrothermal vent at Milos. Marine Chemistry 69, 43–54.